

# Hedgehog signalling within airway epithelial progenitors and in small-cell lung cancer

D. Neil Watkins\*, David M. Berman†‡, Scott G. Burkholder\*, Baolin Wang‡, Philip A. Beachy‡ & Stephen B. Baylin\*

\*Sidney Kimmel Comprehensive Cancer Center, †Department of Pathology, ‡Department of Molecular Biology and Genetics, and Howard Hughes Medical Institute, Johns Hopkins University School of Medicine, Baltimore, Maryland 21231, USA

Embryonic signalling pathways regulate progenitor cell fates in mammalian epithelial development and cancer<sup>1,2</sup>. Prompted by the requirement for sonic hedgehog (Shh) signalling in lung development<sup>3,4</sup>, we investigated a role for this pathway in regeneration and carcinogenesis of airway epithelium. Here we demonstrate extensive activation of the hedgehog (Hh) pathway within the airway epithelium during repair of acute airway injury. This mode of Hh signalling is characterized by the elaboration and reception of the Shh signal within the epithelial compartment, and immediately precedes neuroendocrine differentiation. We reveal a similar pattern of Hh signalling in airway development during normal differentiation of pulmonary neuroendocrine precursor cells, and in a subset of small-cell lung cancer (SCLC), a highly aggressive and frequently lethal human tumour with primitive neuroendocrine features. These tumours maintain their malignant phenotype *in vitro* and *in vivo* through ligand-dependent Hh pathway activation. We propose that some

types of SCLC might recapitulate a critical, Hh-regulated event in airway epithelial differentiation. This requirement for Hh pathway activation identifies a common lethal malignancy that may respond to pharmacological blockade of the Hh signalling pathway.

Sonic hedgehog (Shh), a mammalian hedgehog (Hh) pathway ligand, mediates epithelial–mesenchymal interactions in lung development by signalling to adjacent lung mesenchyme, as indicated by expression of the Hh receptor and pathway target *Patched* (*Ptch*)<sup>5</sup>. Loss of Shh function results in severe lung defects associated with failure of branching morphogenesis<sup>3,4</sup>. As developmental pathways regulate progenitor cell fates and differentiation in some regenerating mammalian epithelia<sup>1,2</sup>, we hypothesized that Hh signalling might be important in airway epithelial repair.

In contrast to the skin and colon, adult airway epithelium rarely proliferates unless injured<sup>6</sup>. To uncover a role for Hh signalling in this process, we studied a mouse model of acute airway repair in which Clara cells, specialized airway epithelial cells predominant in distal conducting airways, are depleted within 24 h of systemic naphthalene administration<sup>6</sup>. Activation of a putative airway progenitor results in epithelial regeneration within three days, with increased numbers of airway neuroendocrine cells—a normally rare cell type implicated in the regulation of airway epithelial growth and development<sup>6,7</sup>. In regenerating airways, we observed marked expression of both Shh ligand and Gli1, a transcriptional target of Hh signalling<sup>8</sup>, in the epithelial compartment 72 h after naphthalene injury (Fig. 1a). By day 4, Gli1 was not observed in nascent airway epithelial cells expressing calcitonin gene-related peptide (CGRP), a marker of neuroendocrine differentiation (Fig. 1a, b). These data show that acute airway epithelial regeneration results in widespread activation of airway intraepithelial Hh signalling, which

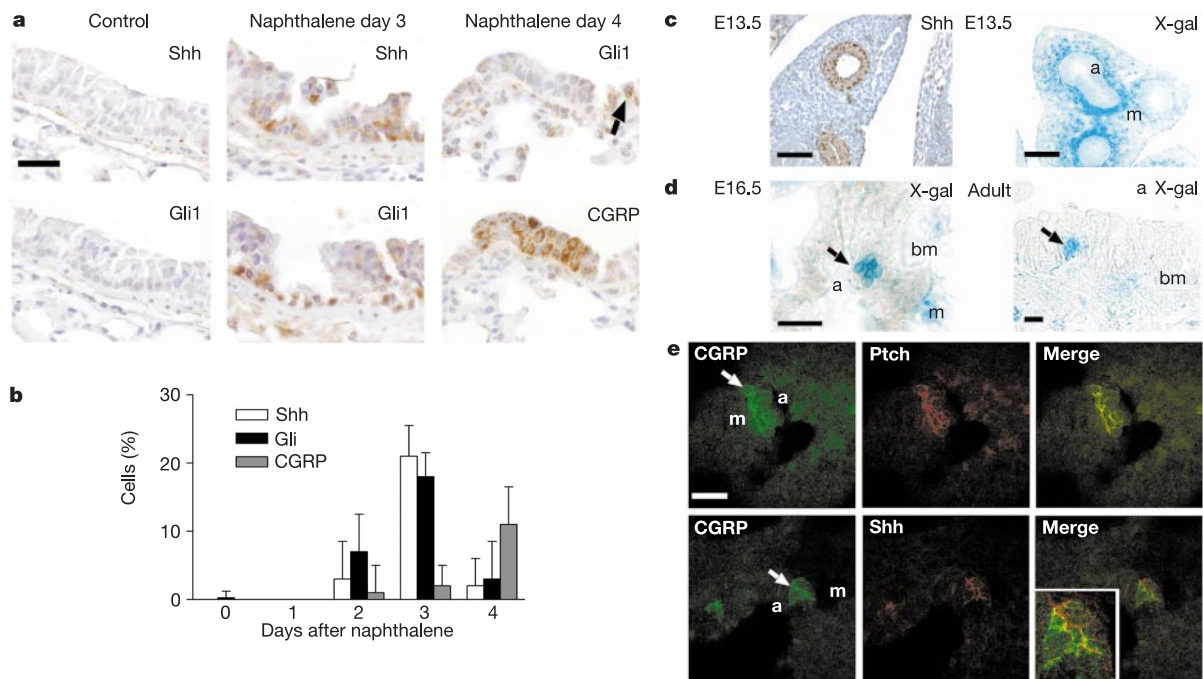


**Figure 1** Hedgehog signalling in airway repair and development. **a**, Immunohistochemical detection of Shh and Gli1 in adult mouse airways is negative in normal airways (left panels), but positive for both Shh and Gli1 in serial sections 3 days after naphthalene injury (middle panels). By 4 days after naphthalene treatment (right panels), Gli1-positive cells are reduced in number (arrow). Serial sections demonstrate that nascent CGRP-positive cells do not express stained Gli1. Scale bar, 50  $\mu$ m. **b**, Quantitative analysis of bronchial epithelial staining in **a** ( $n = 4$ , mean  $\pm$  s.e.m.). **c**, Shh signalling in E13.5 lungs. Shh immunostaining in embryonic airway epithelium is shown in the left panel. The

right panel shows X-gal staining of lungs obtained from E13.5 *Ptch-LacZ* mouse embryos, demonstrating intense mesenchymal staining. Scale bar, 25  $\mu$ m. **d**, Clusters of LacZ-positive cells (arrows) are seen in the airway epithelium of E16.5 (left panel) and adult (right panel) mice. Scale bar, 25  $\mu$ m. a, airway; m, mesenchyme; bm, basement membrane. **e**, Confocal immunofluorescence detection of Hh signalling in lung development. The top row demonstrates expression of both CGRP and Ptch in an E16.5 airway (arrow), similar to that shown in **d**. The bottom row shows expression of CGRP (arrow) adjacent to Shh-expressing epithelial cells (see high-magnification inset). Scale bar, 25  $\mu$ m.

immediately precedes neuroendocrine differentiation.

Embryonic lung epithelial cells express Shh, which is thought to signal to adjacent lung mesenchyme to regulate branching morphogenesis<sup>3-5</sup>. In light of this, our detection of Shh and Gli1 within the epithelial compartment during airway epithelial regeneration was unexpected. To determine whether such intraepithelial signalling occurred in embryonic lung development, we studied mice in which one copy of *Ptch* is replaced in-frame with the  $\beta$ -galactosidase ( $\beta$ -gal) gene by homologous recombination<sup>9</sup>. As *Ptch* is a transcriptional target of the Gli proteins, expression of  $\beta$ -gal indicates activation of the Hh pathway<sup>9,10</sup>. Early gestation (embryonic day (E)13.5) embryos showed expression of Shh protein in the primitive lung endoderm, and intense  $\beta$ -gal expression in the adjacent mesenchyme (Fig. 1c). By contrast, later lung development (E16.5) was characterized by clusters of  $\beta$ -gal-expressing cells in the developing airway epithelium (Fig. 1d). Small numbers of cells expressing  $\beta$ -gal persist in the basal layer of the adult bronchial epithelium (Fig. 1d). Similar clusters of epithelial cells expressing the neuroendocrine marker CGRP and *Ptch* were observed by confocal immunofluorescence in E16.5 airways, immediately adjacent to cells expressing Shh (Fig. 1e). These data suggest that during normal development, neuroendocrine precursors within the airway epithelial compartment respond to a Shh signal elaborated by adjacent airway epithelial cells.

SCLC is an aggressive, highly lethal malignancy with primitive neuroendocrine features<sup>11</sup>. As aberrant reactivation of developmental pathways may have a role in cancer growth<sup>1,2</sup>, we wondered whether the epithelial Hh signalling we had observed in airway embryogenesis and repair might persist in SCLC. Analysis of SCLC tissue showed that five out of ten tumours expressed both Shh and Gli1 (Fig. 2a; see also Supplementary panel a). Out of 40 non-SCLC (NSCLC) tumours, nine demonstrated Shh expression and of

these, four demonstrated co-expression of Gli1 (Fig. 2a; see also Supplementary panel a). These data provide indirect evidence of persistent activation of Hh signalling in lung cancer, predominantly in SCLC. These findings were confirmed by analysis of human lung cancer cell lines. Notably, all seven SCLC and seven NSCLC cell lines expressed Shh protein (Fig. 2b). Out of five breast and eight colon cancer cell lines examined, only one (CACO2) expressed Shh protein, and none expressed Gli1 protein, as shown by western blot analysis (data not shown). Importantly, expression of both Shh and Gli1 proteins was observed in five out of seven SCLC lines, and this correlated with increased expression of *Ptch* messenger RNA (Fig. 2b). In contrast, NSCLC lines expressed Shh and low levels of *Ptch*, but not Gli1. These data are summarized in Supplementary panel b.

To determine how Hh signalling might function in these tumours, we co-cultured cancer cells with Shh-LIGHT2 cells, a fibroblast reporter cell line that responds to exogenous Shh by activation of an integrated Gli-responsive luciferase reporter<sup>10</sup>. Some NSCLC cells that express Shh are capable of heterologous cell signalling to the reporter cell line (Fig. 2c), suggesting that NSCLC retains the Shh export properties of primitive lung endodermal cells that signal to adjacent mesenchymal cells in early development. By contrast, the SCLC cells we studied display a marked reduction in this ability to signal to adjacent cells. These data demonstrate that distinct types of lung cancer cells recapitulate different aspects of Shh signalling seen in lung development and repair.

We next addressed the mechanism of Hh pathway activation in SCLC. Dual-label immunostaining for Shh and Gli1 in SCLC nude mouse xenografts demonstrated Shh-expressing cells adjacent to Gli1-expressing cells (Fig. 2d). These data suggest juxtacrine Hh pathway activation in SCLC markedly similar to that observed in

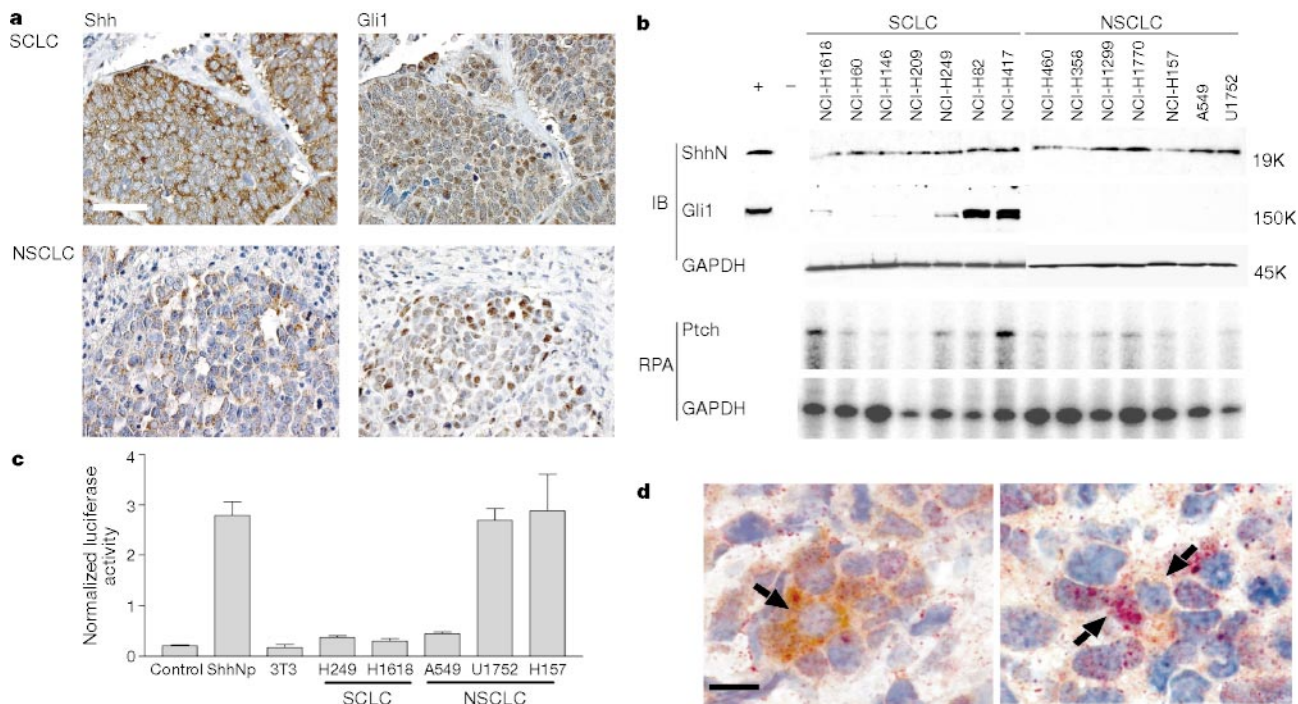


**Figure 2** Hh signalling in lung cancer. **a**, Examples of Shh and Gli1 immunostaining in human lung cancer tissue. Note the widespread co-expression of Shh and Gli1 in SCLC, which is reduced in the NSCLC example. **b**, Expression of Hh signalling components in lung cancer cell lines. The top panel shows immunoblotting (IB) data for expression of Shh, Gli1 and GAPDH. The bottom panel demonstrates *Ptch* mRNA expression in the same cell lines detected by RNase protection assay (RPA). The markers along the right indicate relative molecular mass. **c**, Induction of *Gli-luciferase* activity in Shh-LIGHT2 reporter cells

co-cultured with purified Shh-Np or the cell lines indicated on the x axis. Luciferase activity is normalized to a Renilla luciferase internal control ( $n = 6$ , mean  $\pm$  s.e.m.). **d**, Shh and Gli1 expression in NCI-H249 SCLC xenograft cells detected by dual-label immunohistochemistry. Brown, Shh; red, Gli1. The left panel shows a tumour cell expressing Shh alone (arrow); the right panel shows a Shh-expressing tumour cell (top arrow) and an adjacent Gli1-expressing tumour cell (bottom arrow).

airway development and repair. Next, we asked whether ligand-driven Hh pathway activation promotes growth of SCLC. Inhibition of Shh ligand activity in NCI-H249 and NCI-H1618 SCLC cells with the 5E1 Shh-N monoclonal antibody<sup>12</sup> resulted in growth inhibition (Fig. 3a). Although NCI-H157 NSCLC cells express Shh, they do not express Gli1 protein, and are not affected by 5E1 treatment (Fig. 3a). These data demonstrate that growth of SCLC cells *in vitro* is dependent on ligand-mediated activation of the Hh pathway, and suggest the presence of a normal Ptch receptor, confirmed by sequencing of *Ptch* complementary DNA in both NCI-H249 and NCI-H1618 SCLC cells generated by reverse transcription-polymerase chain reaction (RT-PCR) (data not shown).

The *Veratrum* alkaloid cyclopamine specifically inhibits the Hh pathway<sup>10,13,14</sup> through interaction with the Hh signalling protein smoothed<sup>15,16</sup>. Moreover, cyclopamine blocks the oncogenic effects of mutations of *Ptch* in fibroblasts<sup>10</sup>, and inhibits the malignant growth of medulloblastoma cells lacking *Ptch* function<sup>17</sup>. Treatment of NCI-H249 SCLC cells with cyclopamine, or a more potent analogue KAAD-cyclopamine<sup>10</sup>, resulted in significant growth inhibition, whereas tomatidine, a closely related compound that lacks the capacity to inhibit Hh signalling, had no effect (Fig. 3b). The effects of cyclopamine and KAAD-cyclopamine on the growth of SCLC reflect their relative potency in silencing Hh pathway activation *in vitro*<sup>10</sup>. None of KAAD-cyclopamine, cyclopamine or tomatidine was able to affect growth of NCI-H157 NSCLC cells (Fig. 3c). The growth-inhibitory effect of cyclopamine, if due to Hh pathway blockade, should be bypassed by constitutive overexpression of the Hedgehog pathway effector Gli1 (ref. 17). We indeed observed that stable expression of a Flag-tagged Gli1 protein<sup>18</sup> protected NCI-H249 SCLC cells from growth inhibition by cyclopamine, whereas a Gli1 mutant lacking the zinc finger DNA-binding domain had no effect (Fig. 3d). Treatment of nine cancer cell lines with cyclopamine at concentrations up to 10  $\mu$ M demonstrated growth inhibition only in SCLC cells that expressed both Shh and its transcriptional effector Gli1 (Supplementary panel b). These data show that cyclopamine induces growth inhibition in SCLC cells expressing both Shh and Gli1 by specific inhibition of the Hh pathway.

We next investigated the relationship between Hh pathway blockade by cyclopamine and growth arrest in SCLC. Unsynchronized NCI-H249 SCLC cells treated with 5  $\mu$ M cyclopamine for 72 h demonstrated arrest of the cell cycle in Go/G1 (Fig. 3e) and apoptosis indicated by an increase in cleaved PARP (Fig. 3f). Analysis of *Ptch* mRNA expression revealed downregulation in response to cyclopamine treatment (Fig. 3g). These results indicate silencing of Hh pathway activation at concentrations of cyclopamine that induce both growth arrest and apoptosis. We next investigated the possibility that SCLC cells might express transcripts indicative of a progenitor cell phenotype. We detected expression of BMP4, a morphogen and putative target of Hh expressed in lung epithelial embryogenesis<sup>19</sup>, and nestin, an intermediate filament characteristic of neural stem cells in medulloblastoma<sup>17</sup> (Fig. 3h). Treatment of NCI-H249 SCLC cells with cyclopamine for 48 h inhibited expression of both these genes (Fig. 3h), as well as the expression of human ASH-1, a transcription factor required for pulmonary neuroendocrine differentiation<sup>20</sup>. These changes in gene expression suggest that Hh signalling maintains a progenitor cell fate in SCLC.

Pathological activation of Hh signalling is associated with medulloblastoma, a malignant brain tumour thought to arise from the granule cells of the cerebellum<sup>9,21</sup>. Maintenance of abnormal progenitor-like fates through continued Hh pathway activation is essential for malignant growth of these tumours *in vivo*<sup>17</sup>. We wondered whether SCLC cells were similarly dependent on Hh signalling for their malignant behaviour. NCI-H249 SCLC cells treated with cyclopamine showed reduced soft agar clonogenicity—an *in vitro* assay of tumorigenicity (Fig. 4a, b). This effect was

reversed in cells overexpressing the Hh pathway transcriptional effector Gli1 (Fig. 4a, b). We next tested the ability of systemic cyclopamine treatment to inhibit the growth of SCLC xenografts in nude mice. Mice bearing xenografts were treated subcutaneously

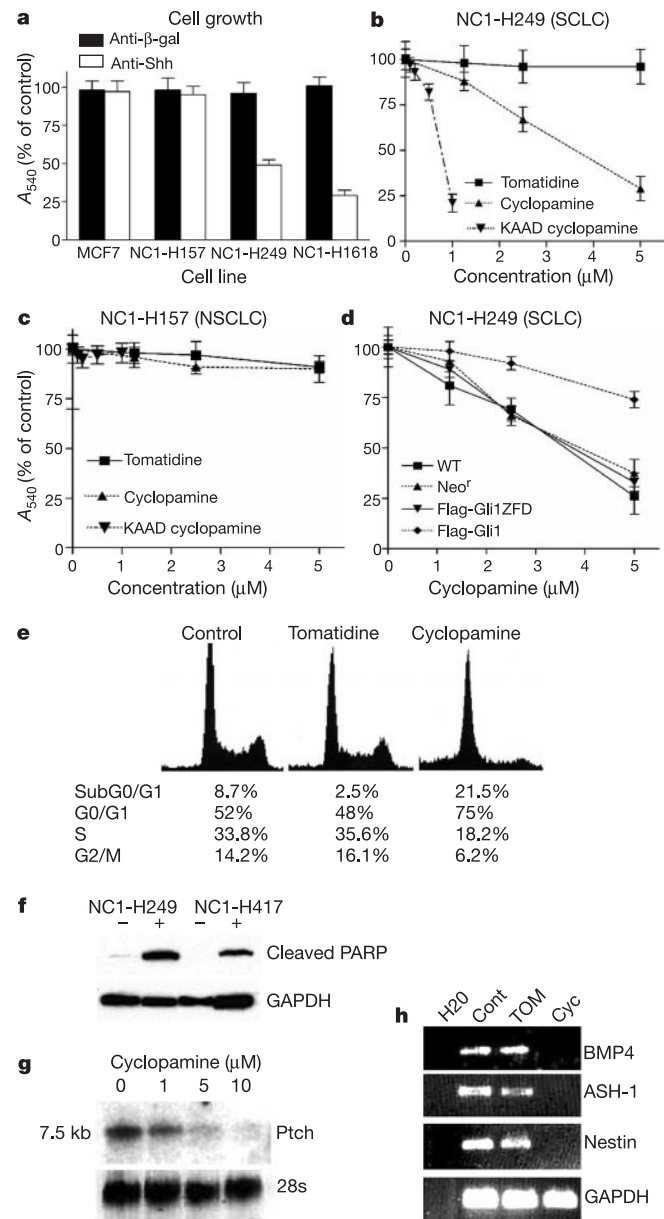


**Figure 3** Hh pathway activation is essential for the growth of SCLC. **a**, Growth of cancer cell lines treated with monoclonal antibodies against  $\beta$ -galactosidase ( $\beta$ -gal) as a control, or Shh for 4 days. **b**, NCI-H249 SCLC cell growth after 5 days, treated with tomatidine, cyclopamine or KAAD cyclopamine at the indicated concentrations. **c**, Identical experiment performed in NCI-H157 NSCLC cells. **d**, Response of stably transfected NCI-H249 SCLC cells to treatment with cyclopamine when expressing neomycin resistance (*Neo<sup>r</sup>*), a mutant Gli1 lacking the zinc finger domain (Flag-Gli1ZFD), Gli1 (Flag-Gli1), and wild-type untransfected (WT) cells. Cell viability was measured by MTT assay, detected at an absorbance at 540 nm ( $A_{540}$ ) ( $n = 6$ ) and expressed as a percentage of control  $\pm$  s.e.m. **e**, Cell cycle analysis in NCI-H249 cells treated with tomatidine or cyclopamine (5  $\mu$ M). Percentages in each phase of the cell cycle are shown below and are shown as the mean of three experiments. **f**, Cleaved PARP expression in NCI-H249 and NCI-H417 SCLC cells treated with tomatidine (–) or cyclopamine (+) (5  $\mu$ M). **g**, *Ptch* mRNA expression in NCI-H249 SCLC cells detected by northern blot analysis after treatment with cyclopamine. 28s RNA stained with ethidium bromide is shown as a loading control. **h**, RT-PCR analysis of transcripts in NCI-H249 SCLC cells. Cont, control; Tom, tomatidine treated; Cyc, cyclopamine treated.

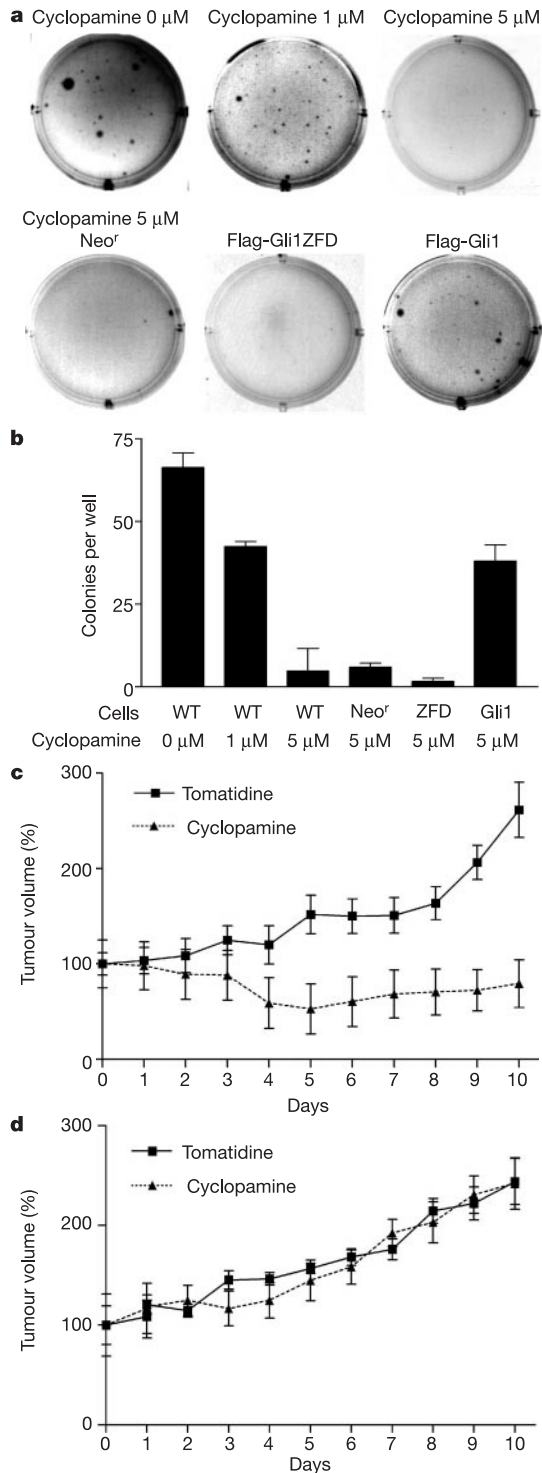


**Figure 4** Cyclopamine inhibits SCLC tumorigenicity. **a**, The top panel shows soft agar growth of NCI-H249 SCLC cells treated with cyclopamine. Plates were stained with ethidium bromide. The bottom panel shows colony formation of NCI-H249 SCLC cells treated with cyclopamine (5 μM) and stably transfected with neomycin resistance (Neo<sup>r</sup>), mutant Gli1 (Flag-Gli1ZFD) or Gli1 (Flag-Gli1). **b**, Quantitative analysis of the experiment described in **a**. Data are shown as mean colonies per well ± s.e.m. (*n* = 6). **c**, Growth of NCI-H249 nude mouse subcutaneous xenografts in animals treated with tomatidine or cyclopamine for 10 days. **d**, Identical experiment to that shown in **c** except that A549 NSCLC cells were used. Data are shown as mean tumour volume ± s.e.m. as a percentage of tumour volume at day 0 (*n* = 7).

with 25 mg<sup>-1</sup> kg<sup>-1</sup> day<sup>-1</sup> cyclopamine as described<sup>17</sup>. Growth inhibition was observed in three SCLC lines: NCI-H249 (Fig. 4c), as well as NCI-H417 and NCI-H1618 (data not shown). No effect was observed in A549 NSCLC cells (Fig. 4d) nor in HCT-116 colon cancer xenografts (data not shown). These data are summarized in Supplementary panel b, and show that Hh signalling is required for the growth *in vivo* of SCLC cells that express both Shh and Gli1.

We have shown that Hh signalling in airway epithelium is not limited to epithelial–mesenchymal interactions, but can be contained within the airway epithelial compartment during embryonic neuroendocrine differentiation and airway repair. Taking evidence that links Hh signalling to cerebellar progenitor cell differentiation into consideration<sup>21–23</sup>, we propose a similar role for this pathway in the regulation of airway progenitor cell fates, which may be specified immediately before the divergence of neuroendocrine and non-neuroendocrine lineages. The dependency of SCLC cells on Hh pathway activation is also notable in that it relies on the presence of Shh ligand, it occurs in the absence of mutations in *Ptch*, and recapitulates juxtacrine Hh signalling seen in development and airway repair. SCLC may represent a malignancy arising from an airway epithelial progenitor that retains both Hh signalling and primitive features of pulmonary neuroendocrine differentiation. The vulnerability of SCLC to Hh pathway blockade may represent a new therapeutic approach to a disease with a poor prognosis<sup>24</sup>. □

**Methods**

**Detection of β-gal expression**

*Ptch-LacZ* mice were maintained and genotyped as described<sup>9</sup>. 5-bromo-4-chloro-3-indolyl-β-D-galactoside (X-gal) staining in microdissected mouse lungs was performed overnight as described<sup>25</sup>, followed by post-fixation in formalin, paraffin embedding and sectioning. We used wild-type littermates as negative controls.

**Immunohistochemistry**

Single-colour DAB-immunoperoxidase staining was performed using a modification of the DAKO CSA system. Detailed protocols are available on request. Antibodies were from Santa Cruz Biotechnologies: Shh (N-19; sc-1194); Gli1 (N-16; sc-6153); CGRP (N-20; sc-8856). Shh, Ptch and Gli1 staining was optimized on paraffin sections from Shh wild-type and knockout embryos. Gli1 staining was further confirmed in Flag-Gli1-overexpressing Cos-7 cells by immunofluorescence. Peptide competition ablated staining in tumour samples and embryos. Dual-colour immunohistochemistry was performed using the DAKO Envision system. Dual-colour immunofluorescence was performed on fresh-frozen sections fixed in paraformaldehyde using Molecular Probes Alexa secondary antibodies.

**Western immunoblot**

Whole-cell lysates were sonicated in 2% SDS/50 mM TrisHCl, pH 8. Western blot using rabbit polyclonal antibodies for Shh-N were performed as described<sup>26</sup>. A rabbit polyclonal antibody to Gli1 was developed as described<sup>27</sup> using a glutathione S-transferase fusion protein containing amino acid residues 216–271 of human Gli1. Anti-cleaved PARP was obtained from Promega.

**RNAse protection assay and northern blot analysis**

RNAse protection assay (RPA) was performed as described<sup>28</sup> using a *Ptch*-specific antisense RNA probe corresponding to bases 1338–1788 of the human patched-1 cDNA (GI:1335863) generated by RT-PCR and subcloned into pCR-TOPOII (Stratagene). Northern blotting of 10 μg total RNA was performed as described<sup>29</sup>, and probed with a *Ptch*-specific cDNA probe obtained from the same construct.

**RT-PCR**

Total cellular RNA was treated with DNase, reverse transcribed, and amplified for 31 cycles at an annealing temperature of 55 °C. Primers used were BMP4(+), 5'-CTTTACCGGC TTCAGTCTGGG-3'; BMP4(-), 5'-CCCAATCCCACTCCCTTGAG-3'; GAPDH(+), 5'-ATCTCCAGGAGCGAGATCCC-3'; GAPDH(-), 5'-CGTTCGGCTCAGGGATGA CCT-3'; ASH-1(+), 5'-CGCATGGAAAGCTCTGCCAAG-3'; ASH-1(-), 5'-TGACC AACTTGACGCGGTTGC-3'; nestin(+), 5'-CTCTGGGAGAGGATCAAG-3'; nestin(-), 5'-CCTTTGTGACAGGCTCAGTG-3'.

**Shh-LIGHT2 reporter assay**

Superconfluent reporter cells were cultured as described<sup>10</sup>, then co-cultured in low serum conditions in the presence of 1 × 10<sup>5</sup> cells per well of the cell line of interest or purified Shh-Np<sup>10</sup>. Luciferase and Renilla luciferase assays were performed using the Promega Dual Luciferase Reporter Assay system.

**Cell culture experiments**

Cell lines were obtained from American Type Culture Collection (ATCC). Shh inhibitor experiments were performed in 0.5% calf serum. Cyclopamine was obtained from

Toronto Research Chemicals. Both were dissolved as  $\times 1,000$  stocks in DMSO medium. Flag-tagged Gli1 vectors were obtained from the Joyner laboratory<sup>18</sup>. To generate NCI-H249 SCLC cells overexpressing each of the Gli vectors, mass cultures were stably co-transfected using lipofectamine (Invitrogen) with the Flag-Gli vector of interest, and pcDNA3.1 (Stratagene) to confer neomycin resistance. 5E1 anti-ShhN monoclonal antibody was used at a concentration of  $10 \mu\text{g ml}^{-1}$  as described<sup>12</sup>. Soft agar assays were performed as described<sup>10</sup>. Cells were seeded into six-well plates at a density of 20,000 cells per well in agar containing 2% calf serum. MTT assays were performed as described<sup>28</sup>.

**Nude mouse xenografts**

Tumour cell lines were injected subcutaneously at  $1 \times 10^7$  cells per mouse and allowed to grow to a maximum diameter of 5 mm. Cyclopamine was administered as described<sup>17</sup>. Tumours were measured daily and the tumour volume calculated as described<sup>30</sup>.

Received 1 November 2002; accepted 12 February 2003; doi:10.1038/nature01493.  
Published online 5 March 2003.

1. Reya, T., Morrison, S. J., Clarke, M. F. & Weissman, I. L. Stem cells, cancer, and cancer stem cells. *Nature* **414**, 105–111 (2001).
2. Taipale, J. & Beachy, P. A. The Hedgehog and Wnt signalling pathways in cancer. *Nature* **411**, 349–354 (2001).
3. Pevicelli, C. V., Lewis, P. M. & McMahon, A. P. Sonic hedgehog regulates branching morphogenesis in the mammalian lung. *Curr. Biol.* **8**, 1083–1086 (1998).
4. Litingtung, Y., Lei, L., Westphal, H. & Chiang, C. Sonic hedgehog is essential to foregut development. *Nature Genet.* **20**, 58–61 (1998).
5. Bellusci, S. *et al.* Involvement of Sonic hedgehog (Shh) in mouse embryonic lung growth and morphogenesis. *Development* **124**, 53–63 (1997).
6. Reynolds, S. D., Giangreco, A., Power, J. H. & Stripp, B. R. Neuroepithelial bodies of pulmonary airways serve as a reservoir of progenitor cells capable of epithelial regeneration. *Am. J. Pathol.* **156**, 269–278 (2000).
7. Peake, J. L., Reynolds, S. D., Stripp, B. R., Stephens, K. E. & Pinkerton, K. E. Alteration of pulmonary neuroendocrine cells during epithelial repair of naphthalene-induced airway injury. *Am. J. Pathol.* **156**, 279–286 (2000).
8. Lee, J., Platt, K. A., Censullo, P. & Ruiz i Altaba, A. Gli1 is a target of Sonic hedgehog that induces ventral neural tube development. *Development* **124**, 2537–2552 (1997).
9. Goodrich, L. V., Milenkovic, L., Higgins, K. M. & Scott, M. P. Altered neural cell fates and medulloblastoma in mouse patched mutants. *Science* **277**, 1109–1113 (1997).
10. Taipale, J. *et al.* Effects of oncogenic mutations in Smoothened and Patched can be reversed by cyclopamine. *Nature* **406**, 1005–1009 (2000).
11. Zochbauer-Muller, S., Gazdar, A. F. & Minna, J. D. Molecular pathogenesis of lung cancer. *Annu. Rev. Physiol.* **64**, 681–708 (2002).
12. Ericson, J., Morton, S., Kawakami, A., Roelink, H. & Jessell, T. M. Two critical periods of Sonic Hedgehog signaling required for the specification of motor neuron identity. *Cell* **87**, 661–673 (1996).
13. Incardona, J. P., Gaffield, W., Kapur, R. P. & Roelink, H. The teratogenic Veratrum alkaloid cyclopamine inhibits sonic hedgehog signal transduction. *Development* **125**, 3553–3562 (1998).
14. Cooper, M. K., Porter, J. A., Young, K. E. & Beachy, P. A. Teratogen-mediated inhibition of target tissue response to Shh signaling. *Science* **280**, 1603–1607 (1998).
15. Chen, J. K., Taipale, J., Cooper, M. K. & Beachy, P. A. Inhibition of Hedgehog signaling by direct binding of cyclopamine to Smoothened. *Genes Dev.* **16**, 2743–2748 (2002).
16. Chen, J. K., Taipale, J., Young, K. E., Maiti, T. & Beachy, P. A. Small molecule modulation of Smoothened activity. *Proc. Natl Acad. Sci. USA* **99**, 14071–14076 (2002).
17. Berman, D. M. *et al.* Medulloblastoma growth inhibition by Hedgehog pathway blockade. *Science* **297**, 1559–1561 (2002).
18. Park, H. L. *et al.* Mouse Gli1 mutants are viable but have defects in SHH signaling in combination with a Gli2 mutation. *Development* **127**, 1593–1605 (2000).
19. Weaver, M., Yingling, J. M., Dunn, N. R., Bellusci, S. & Hogan, B. L. Bmp signaling regulates proximal-distal differentiation of endoderm in mouse lung development. *Development* **126**, 4005–4015 (1999).
20. Borges, M. *et al.* An achaete-scute homologue essential for neuroendocrine differentiation in the lung. *Nature* **386**, 852–855 (1997).
21. Kenney, A. M. & Rowitch, D. H. Sonic hedgehog promotes G(1) cyclin expression and sustained cell cycle progression in mammalian neuronal precursors. *Mol. Cell Biol.* **20**, 9055–9067 (2000).
22. Dahmane, N. & Ruiz-i-Altaba, A. Sonic hedgehog regulates the growth and patterning of the cerebellum. *Development* **126**, 3089–3100 (1999).
23. Wechsler-Reya, R. J. & Scott, M. P. Control of neuronal precursor proliferation in the cerebellum by Sonic Hedgehog. *Neuron* **22**, 103–114 (1999).
24. Johnson, D. H. Management of small cell lung cancer\*: current state of the art. *Chest* **116**, 525S–530S (1999).
25. Hogan, B. L., Beddington, R., Constantini, F. & Lacy, E. *Manipulating the Mouse Embryo* (Cold Spring Harbor Press, Plainview, 1994).
26. Chang, D. T. *et al.* Products, genetic linkage and limb patterning activity of a murine hedgehog gene. *Development* **120**, 3339–3353 (1994).
27. Wang, B., Fallon, J. F. & Beachy, P. A. Hedgehog-regulated processing of Gli3 produces an anterior/posterior repressor gradient in the developing vertebrate limb. *Cell* **100**, 423–434 (2000).
28. Sriuranpong, V. *et al.* Notch signaling induces rapid degradation of achaete-scute homolog 1. *Mol. Cell Biol.* **22**, 3129–3139 (2002).
29. Nakakura, E. K. *et al.* Mammalian Scratch: a neural-specific Snail family transcriptional repressor. *Proc. Natl Acad. Sci. USA* **98**, 4010–4015 (2001).
30. Park, B. H., Vogelstein, B. & Kinzler, K. W. Genetic disruption of PPARdelta decreases the tumorigenicity of human colon cancer cells. *Proc. Natl Acad. Sci. USA* **98**, 2598–2603 (2001).

**Acknowledgements** We acknowledge M. Scott for the donation of the *Ptch-LacZ* mice; A. Joyner for the Flag-Gli1 expression vectors; J. Chen for the gift of KAAD cyclopamine; J. Taipale, S. Karhadkar, B. Nelkin and K. Schuebel for discussions; and E. Gabrielson for help in obtaining lung cancer tissue. We also thank K. Young and L. Meszler and the Sidney Kimmel Comprehensive Cancer Center Cell Imaging Facility for technical assistance. This work is supported by the Flight Attendant Medical Research Institute and the NCI/SPOR. P.A.B. is an investigator of the Howard Hughes Medical Institute.

**Competing interests statement** The authors declare competing financial interests: details accompany the paper on Nature’s website (♦ <http://www.nature.com/nature>).

**Correspondence** and requests for materials should be addressed to D.N.W. (e-mail: nwatkins@jhmi.edu).

.....  
**Links between signal transduction, transcription and adhesion in epithelial bud development**

**Colin Jamora\*, Ramanuj DasGupta\*†, Pawel Kocieniewski\* & Elaine Fuchs\***

\* Howard Hughes Medical Institute, Laboratory of Mammalian Cell Biology and Development, The Rockefeller University, New York, New York 10021, USA

The morphogenesis of organs as diverse as lungs, teeth and hair follicles is initiated by a downgrowth from a layer of epithelial stem cells<sup>1,2</sup>. During follicular morphogenesis, stem cells form this bud structure by changing their polarity and cell–cell contacts. Here we show that this process is achieved through simultaneous receipt of two external signals: a Wnt protein to stabilize  $\beta$ -catenin, and a bone morphogenetic protein (BMP) inhibitor to produce Lef1.  $\beta$ -Catenin then binds to, and activates, Lef1 transcription complexes that appear to act uncharacteristically by downregulating the gene encoding E-cadherin, an important component of polarity and intercellular adhesion. When either signal is missing, functional Lef1 complexes are not made, and E-cadherin downregulation and follicle morphogenesis are impaired. In *Drosophila*, E-cadherin can influence the plane of cell division and cytoskeletal dynamics<sup>3</sup>. Consistent with this notion, we show that forced elevation of E-cadherin levels block invagination and follicle production. Our findings reveal an intricate molecular programme that links two extracellular signalling pathways to the formation of a nuclear transcription factor that acts on target genes to remodel cellular junctions and permit follicle formation.

During skin development, signals from adjacent epithelial and mesenchymal cells instruct select ectodermal cells to form hair follicle buds. In turn, each bud signals to a small group of underlying mesenchymal cells to condense<sup>1,2</sup>. Once the bud proliferates to form a larger bulb (matrix), it encases this dermal condensate (papilla), and further differentiates into the cells of the hair shaft (Fig. 1a)<sup>1</sup>. Recent evidence suggests that Wnt signalling is involved in this process at a time that correlates with bud-specific patterns of upregulation of P-cadherin and downregulation of E-cadherin<sup>4–9</sup>. Cadherins form the transmembrane core of adherens junctions (AJs) by bridging to  $\alpha$ -catenin and the cytoskeleton through  $\beta$ -catenin, a protein which on its own is prone to degradation<sup>10,11</sup>.  $\beta$ -Catenin’s degradation machinery is transiently suppressed by Wnt signalling. This renders  $\beta$ -catenin a new-found stability and function, binding to and activating members of the

**Supplementary Information** accompanies the paper on Nature’s website (♦ <http://www.nature.com/nature>).

† Present address: Howard Hughes Medical Institute, Harvard Medical School, Boston, Massachusetts, USA.